DRAFT VERSION DECEMBER 2, 2002
Preprint typeset using LaTeX style emulateapj v. 16/07/00

THE THREE-POINT CORRELATION FUNCTION FOR SPIN-2 FIELDS

MASAHIRO TAKADA AND BHUVNESH JAIN
Department of Physics, University of Pennsylvania, 209 S. 33rd Street, Philadelphia, PA 19104; mtakada,bjain@hep.upenn.edu
Draft version December 2, 2002

ABSTRACT

The three-point correlation function (3PCF) of the spin-2 fields, cosmic shear and microwave background polarization, is a statistical measure of non-Gaussian signals. At each vertex of a triangle, the shear field has two independent components. The resulting eight possible 3PCFs were recently investigated by Schneider & Lombardi (2002) and Zaldarriaga & Scoccimarro (2002). Using rotation and parity transformations they posed the question: how many components of the shear 3PCF are non-zero and useful? We address this question using an analytical model and measurements from ray-tracing simulations. We show that all the eight 3PCFs are generally non-zero and have comparable amplitude. These eight 3PCFs can be used to improve the signal-to-noise from survey data and their configuration dependence can be used to separate the contribution from E- and B-modes. This separation provides a new and precise probe of systematic errors. We estimate the signal-to-noise for measuring the shear 3PCF from weak lensing surveys using simulated maps that include the noise due to intrinsic ellipticities. A deep lensing survey with area of order 10 square degrees would allow for the detection of the shear 3PCFs; a survey with area exceeding 100 square degrees is needed for accurate measurements.

Subject headings: cosmology: theory – gravitational lensing – large-scale structure of universe – cosmic microwave background

1. INTRODUCTION

Can the three-point correlation function (3PCF) of a spin-2 field be a useful probe of non-Gaussian signals in cosmology? Most previous work has focused on the 3PCF or its Fourier transform, the bispectrum, of scalar quantities such as the galaxy number density and temperature anisotropies in the cosmic microwave background (CMB). An exciting development is the recent detection of the 3PCF of the cosmic shear field by Bernardeau, Mellier & Van Waerbeke (2002a; also see Bernardeau, Van Waerbeke & Mellier 2002b), which provides new constraints on structure formation models beyond those provided by two-point statistics. For the CMB, the bispectrum of the temperature anisotropies is a promising way of probing primordial non-Gaussian perturbations (e.g., Verde et al. 2000; Komatsu et al. 2002). The 3PCF of the CMB polarization might open a new, complementary window for this in that it can separately measure the non-Gaussian signals arising from primordial scalar, vector and tensor perturbations.

A spin-2 field has two components on the sky, hence its 3PCF in general has $2^3 = 8$ components. One may ask: how many of these components are non-zero? Do all components carry useful information about the B- and E-modes of the spin-2 field[1]? Recently, Schneider & Lombardi (2002; hereafter SL02) and Zaldarriaga & Scoccimarro (2002; hereafter ZS02) investigated these questions. The purpose of this *Letter* is to clarify these issues using geometrical arguments and measurements from ray-tracing simulations of the cosmic shear. We will pay particular attention to the problem of how the eight 3PCFs are related to the E- and B-modes.

2. THE 3PCF OF SPIN-2 FIELDS

The two components of a spin-2 field depend on the choice of the coordinate system. Suppose we have the shear components, γ_1 and γ_2 on the sky, for given Cartesian coordinates[2]. A rotation of the coordinate system by φ (in the anticlockwise direction in our convention) transforms the shear fields as $\gamma_1' + i\gamma_2' = (\gamma_1 + i\gamma_2)e^{-i2\varphi}$.

For the two-point correlation function (2PCF), the problem of the coordinate dependence of the shear field has been well studied in the literature (e.g., Bartelmann & Schneider 2001). For a given pair of points, $\mathbf{X}_1$ and $\mathbf{X}_2$, separated by a fixed angle θ, we can define two components of the 2PCF which are invariant under coordinate rotations: $\xi_+(\theta) = \langle\gamma_+(\mathbf{X}_1)\gamma_+(\mathbf{X}_2)\rangle$ and $\xi_\times(\theta) = \langle\gamma_\times(\mathbf{X}_1)\gamma_\times(\mathbf{X}_2)\rangle$. Here $\gamma_+(\mathbf{X}_i)$ and $\gamma_\times(\mathbf{X}_i)$ are the shear components defined by projecting the shear along the direction φ connecting the two points: $\gamma_+(\mathbf{X}_i) + i\gamma_\times(\mathbf{X}_i) = -[\gamma_1(\mathbf{X}_i) + i\gamma_2(\mathbf{X}_i)]\,e^{-2i\varphi}$. The other possible component, $\langle\gamma_+\gamma_\times\rangle$, vanishes because of parity invariance.

SL02 and ZS02 investigated possible eight components of the shear 3PCF based on the $+/\times$ decomposition of the shear field. We will closely follow these authors in setting up the geometry of the 3PCF. In contrast to the 2PCF, there is no unique choice of a reference direction to define the $+/\times$ decompositions for the shear fields at the vertices of a triangle. The 'center of mass', $\mathbf{o}$, of a triangle is one possible fiducial choice: $\mathbf{o} \equiv (1/3)\sum_{i=1}^{3}\mathbf{X}_i$. Figure 1 shows a sketch of the triangle we use to define the shear 3PCFs. The solid and dashed lines at each vertex show the positive directions of the + and $\times$ components, respectively. We also define the interior angle ψ between $\mathbf{x}_1$ and $\mathbf{x}_2$. The projection operator to compute the + or $\times$ components at each vertex is written as:

$$\mathbf{P}_+(\mathbf{X}_i) = -(\theta_{i1}^2 - \theta_{i2}^2, 2\theta_{i1}\theta_{i2})/\theta_i^2,$$
$$\mathbf{P}_\times(\mathbf{X}_i) = -(-2\theta_{i1}\theta_{2i}, \theta_{i1}^2 - \theta_{i2}^2)/\theta_i^2, \quad (1)$$

where $\boldsymbol{\theta}_i \equiv \mathbf{X}_i - \mathbf{o}$. Using these projections, we obtain at each vertex $\gamma_+ = P_{+1}\gamma_1 + P_{+2}\gamma_2$ and $\gamma_\times = P_{\times 1}\gamma_1 + P_{\times 2}\gamma_2$. These transform under parity as $\gamma_+ \to \gamma_+$ and $\gamma_\times \to -\gamma_\times$. In terms of γ_+ and $\gamma_\times$ we define the eight components of the shear 3PCF for a

[1] A two-dimensional spin-2 field can be separated into an E-mode derivable from a scalar potential and a pseudoscalar B-mode (Kamionkowski, Kosowski & Stebbins 1997; Zaldarriaga & Seljak 1997; Hu & White 1997 for the CMB polarization and Stebbins 1996; Kamionkowski et al. 1998; Crittenden et al. 2001; Schneider et al. 2002 for the cosmic shear).

[2] We use the notations of weak lensing for the spin-2 field, γ_i; our discussion can be applied to the CMB polarization if one replaces γ_1 and γ_2 with the Stokes parameters Q and U, respectively.

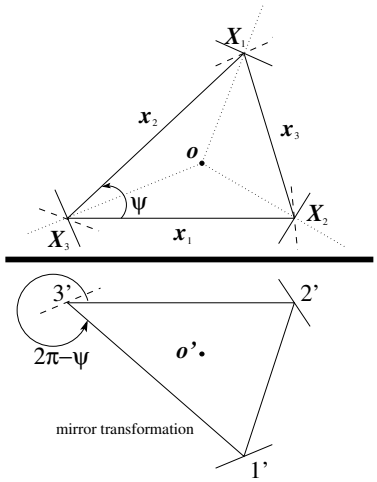

FIG. 1.— *Upper*: Definitions of the triangle variables used for the 3PCF. The interior angle between $\mathbf{x}_1$ and $\mathbf{x}_2$ is defined as ψ and its positive direction is shown by the arrow. Note that the solid and dashed curves at each vertex show the positive directions for γ_+ and $\gamma_\times$. *Lower:* The mirror transformation with respect to the side vector $\mathbf{x}_1$ for $\zeta_{++\times}$. The vertices are transformed as $1 \to 1'$ and so on. Note that the + components remain unchanged in sign, but the sign of the $\times$ component is flipped.

given triangle as a function of x_1, x_2 and ψ:

$$\zeta_{\mu\nu\tau}(x_1,x_2,\psi) \equiv \langle \gamma_\mu(\mathbf{X}_1)\gamma_\nu(\mathbf{X}_2)\gamma_\tau(\mathbf{X}_3)\rangle, \qquad (2)$$

where $\mu,\nu,\tau = +$ or $\times$ and $\langle\cdots\rangle$ denotes the ensemble average. The 3PCF defined above is invariant under triangle rotations with respect to the center **o** as pointed out in SL02. Hence it is fully characterized by the three variables x_1, x_2, ψ, just like the 3PCF of a scalar field (note that if we had used the Cartesian components of the shear, we would need four variables to specify it as it is not invariant under rotation).

For a pure E-mode, based on the properties of γ_+ and $\gamma_\times$ under parity transformations described above, we divide the eight shear 3PCFs into two groups:

$$\text{Parity-even functions: } \zeta_{+++}, \zeta_{+\times\times}, \zeta_{\times+\times}, \zeta_{\times\times+}$$
$$\text{Parity-odd functions: } \zeta_{\times\times\times}, \zeta_{\times++}, \zeta_{+\times+}, \zeta_{++\times}. \qquad (3)$$

Weak lensing only produces the E-mode, while source galaxy clustering, intrinsic alignments and observational systematics induce both E and B–modes in general (Crittenden et al. 2001; Schneider et al. 2002)[3]. For the CMB polarization, although primordial scalar perturbations generate only the E-mode, vector and tensor perturbations can induce both modes (e.g., Kamionkowski et al. 1997).

A question posed by SL02 and ZS02 is whether all eight 3PCFs could have contributions from lensing. We examine this question with geometrical considerations and show results from simulations in the next section. The parity transformation for a triangle can be taken to be a mirror transformation as sketched in Figure 1, which shows the parity transformation with respect to the side vector $\mathbf{x}_1$ as one example. It corresponds to the change $\psi \to 2\pi - \psi$ in our parameters. Figure 1 illustrates the transformation for $\zeta_{++\times}$. From statistical homogeneity and symmetry, the amplitude of the 3PCF depends only on the distances between the center and each vertex. Hence, the absolute amplitudes of $\zeta_{++\times}$ for the two triangles shown should be the same. But the sign of $\gamma_\times$ at the vertex $3'$ changes under this parity transformation. For the eight 3PCFs in equation (3), we can say in general:

$$\text{Parity-even: } \zeta_{\mu\nu\tau}(x_1,x_2,\psi) = \zeta_{\mu\nu\tau}(x_1,x_2,2\pi-\psi),$$
$$\text{Parity-odd: } \zeta_{\mu\nu\tau}(x_1,x_2,\psi) = -\zeta_{\mu\nu\tau}(x_1,x_2,2\pi-\psi). \qquad (4)$$

Next, we consider an isosceles triangle with $x_1 = x_2$. In this case, the $\gamma_\times$ at vertex 3 and $3'$ in Figure 1 are statistically identical (viewed from the center of the triangle, they should have equal contributions when averaged over a matter distribution). We thus have the additional symmetries for the two parity-odd 3PCFs:

$$\zeta_{++\times}(x_1,x_1,\psi) = \zeta_{++\times}(x_1,x_1,2\pi-\psi),$$
$$\zeta_{\times\times\times}(x_1,x_1,\psi) = \zeta_{\times\times\times}(x_1,x_1,2\pi-\psi). \qquad (5)$$

The properties described in equations (4) and (5) lead to

$$\text{Isosceles Triangles: } \zeta_{++\times} = 0, \quad \zeta_{\times\times\times} = 0. \qquad (6)$$

Note that this argument does not lead to the vanishing of the other two parity-odd functions, in which the $\times$ component is at a vertex bounded by unequal sides. For equilateral triangles however all four parity-odd functions vanish:

$$\text{Equilateral Triangles: } \zeta_{\text{parity–odd}} = 0. \qquad (7)$$

We argue that for a generic triangle with all sides unequal, the differences in side lengths break the symmetry that is expressed in equation (5). In other words, the fact that gravitation has a scale dependence allows parity-odd 3PCFs to be non-zero for a triangle with unequal sides. These conclusions are consistent with those of SL02.

3. PREDICTIONS FROM RAY TRACING SIMULATIONS

To demonstrate the properties of the shear 3PCFs more precisely, we employ ray-tracing simulations of the cosmic shear performed by Jain et al. (2000). We use the SCDM model ($\Omega_{\rm m0} = 1$, $h = 0.5$ and $\sigma_8 = 0.6$), with source redshift $z_s = 1$ and area $\Omega_{\rm sky} = 7.68$ degree^2 (see Jain et al. 2000 for more details). We followed Barriga & Gaztañaga (2002) for the algorithm to calculate the 3PCF. Lists of neighbors are used to find the three vertices from the cell-based data as well as to calculate the projection operators for each vertex. The error bars shown in the following figures are computed from 9 different realizations (see Takada & Jain 2002c for more details).

Figure 2 shows the results for the shear 3PCFs for isosceles triangles against the interior angle ψ between the two equal sides $x_1 = x_2 = 0.'97$ (see Figure 1). The shear 3PCF is computed from the simulated data by averaging the estimator over all triplets with given triangle configuration. For the bin size we used $\Delta x = 0.'08$ for the side lengths and $\Delta\psi = \pi/20$ for the interior angle. The upper panel shows the four parity-even 3PCFs, while the lower panel shows the parity-odd functions. As expected, ζ_{+++} appears to have the greatest lensing contributions, and, in particular, peaks for equilateral triangles with $\psi = \pi/3$. The other three modes have smaller amplitude than ζ_{+++}, and two of them are the same because of symmetric triangle and shear configurations. Interestingly, the features of these curves match the theoretical curves shown in Figure 3 of ZS02 (ϕ in their figures corresponds to $\pi - \psi$ in our figure). Their results were presented with arbitrary normalization of the y-axis, so we can only compare the configuration dependence. Thus these small-scale complex features are basically captured by the tangential shear patterns around a single halo.

From the lower panel in Figure 2, it is clear that two of the parity-odd 3PCFs are non-zero, but the others vanish, as stated

[3] Multiple lensing deflections generally induce the B-mode, but Jain, Seljak & White (2000) showed that the induced B-mode is much smaller than the lensing E-mode using ray-tracing simulations.

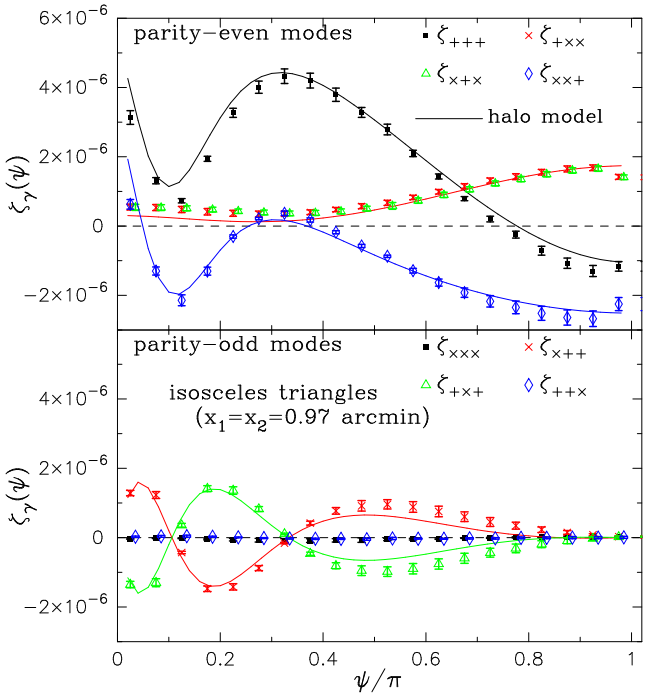

FIG. 2.— Ray-tracing simulation results of the shear 3PCF for isosceles triangles. The two side lengths are $x_1 = x_2 = 0'.97$. The upper panel shows the four parity-even functions, while the lower panel shows the four parity-odd functions. For illustrative purpose, the results for $\zeta_{\times+\times}$ and $\zeta_{++\times}$ are slightly shifted horizontally. The solid curves show analytical calculations of the shear 3PCFs based on the halo model developed in Takada & Jain (2002b).

in equation (6). This result clarifies that the parity-odd 3PCFs in general do carry lensing information and vanish only for special triangle configurations. For isosceles triangles, the two vanishing parity-odd functions can be used to discriminate systematics from the E-mode. For $\psi = \pi/3$, the triangle is equilateral, and all the parity-odd 3PCFs vanish as stated in equation (7).

We have verified that the simulation results are in agreement with the 1-halo term predictions of the halo model. The solid curves in Figure 2 show the halo model predictions that follow the real space halo formalism developed in Takada & Jain (2002b). The calculations are based on adapting equation (52) from this paper by replacing κ_m with the relevant shear component for a halo of given mass. A detailed comparison of analytical and simulation results for different models will be presented in Takada & Jain (2002c).

The features shown above for isosceles triangles are explored for a triangle with three unequal sides in Figure 3, in which $x_1 = x_2/2 = 0'.97$. This figure is plotted over the range $\psi = [0, 2\pi]$ to explicitly show the parity-even (upper panel) and odd (lower panel) properties of the shear 3PCFs. Note that the parity transformation is equivalent to the change $\psi \to 2\pi - \psi$ in our parameters. As noted in ZS02, the amplitude of the 3PCF is suppressed for elongated triangles because of cancellations in the signals by the vector-like property of the shear. The figure reveals that all the parity-odd 3PCFs are non-zero and in fact all the eight 3PCFs have roughly comparable amplitude. Note that $\zeta_{\times\times\times}$ and $\zeta_{+\times+}$ vanish at $\psi/\pi = 0.42$, as the triangle becomes an isosceles triangle with $x_2 = x_3$, and therefore the 3PCFs are consistent with the result in Figure 2.

By rotating the simulated shear field at each position by 45 degrees, we can investigate the 3PCF of a pure B-mode map (Kaiser 1992). Since this procedure transforms $\gamma_+ \to \gamma_\times$ and

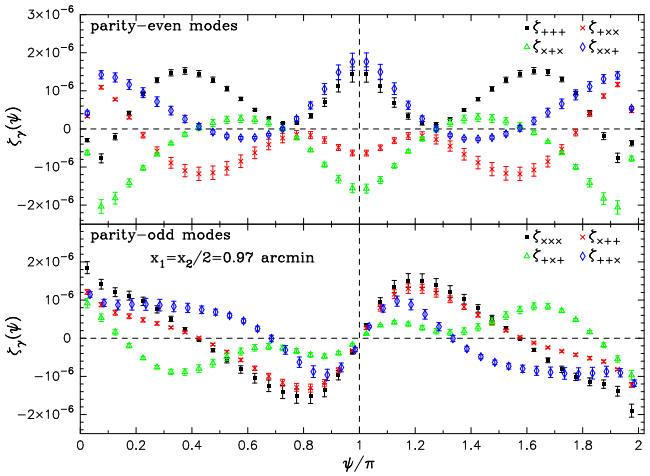

FIG. 3.— The results for a general triangle with $x_1 = x_2/2 = 0'.97$, as in Figure 2.

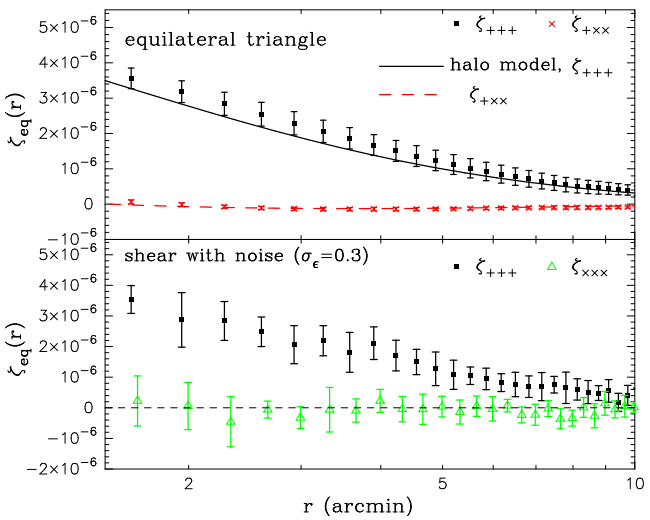

FIG. 4.— The upper panel shows the shear 3PCF for equilateral triangle as a function of the side length. Ray tracing measurements and halo model calculations are shown for the two independent, non-zero 3PCFs, ζ_{+++} and $\zeta_{\times++}$. The lower panel shows ζ_{+++} and $\zeta_{\times\times\times}$ from simulated maps that include noise due to intrinsic ellipticities with rms $\sigma_\epsilon = 0.3$. The bin size is $\Delta r = 0'.325$.

$\gamma_\times \to -\gamma_+$, we find $\zeta^E_{+++} \to \zeta^B_{\times\times\times}$ and so on. Hence, $\zeta^B_{\times\times\times}$ carries most of the B-mode signal for triangles that are close to equilateral. Further the symmetry properties of the 3PCFs under $\psi \to 2\pi - \psi$ (shown in Figure 3) are reversed for the B-mode; for example, $\zeta^B_{\times\times\times}(\psi) = \zeta^B_{\times\times\times}(2\pi - \psi)$. Therefore, we should keep in mind that for a general spin-2 field which includes both E and B modes, the property $\zeta(\psi) = \pm\zeta(2\pi - \psi)$ can no longer be expected. The measurements of ζ thus has to be done for the full range $\psi = [0, 2\pi]$ (unlike the case for the 3PCF of a scalar quantity like the density field or the CMB temperature fluctuations field).

The upper panel of Figure 4 shows the results for the shear 3PCF for equilateral triangles against the side length. For the measurements from simulated data, we used triangles with each side length in the range $[r - \Delta r, r + \Delta r]$, with bin size $\Delta r = 0'.325$ kept fixed. Since all the parity-odd 3PCFs vanish for an equilateral triangle, the results for ζ_{+++} and $\zeta_{+\times\times}$ $(= \zeta_{\times+\times} = \zeta_{+\times\times})$ are shown. We also show the halo model predictions for the 1-halo terms of ζ_{+++} and $\zeta_{+\times\times}$ by the solid and dashed curves, respectively. It is again apparent that the halo model predictions are

in good agreement with the simulation results.

To estimate the signal-to-noise (S/N) for measuring the shear 3PCFs from an actual survey, we need to account for the noise arising from the large intrinsic ellipticities of source galaxies. The lower panel of Figure 4 shows the 3PCFs measured from simulated shear maps including the noise contamination. We assume that the intrinsic ellipticities have random orientations with a Gaussian distribution for the amplitudes with rms $\sigma_\epsilon = 0.3$. The galaxies are taken to be randomly distributed with number density $n_{\rm gal} \approx 38$ arcmin^{-2}. One can see that ζ_{+++} can be detected from a survey with area of order 10 square degrees, provided the errors are dominated by statistical errors. The other 3PCFs are more difficult to measure for equilateral triangles. Here we also show $\zeta_{\times\times\times}$ which is expected to be zero for an E-mode signal, so the error bars on it show the accuracy with which the B-mode can be constrained. These results in part verify the detection of the shear 3PCF by Bernardeau et al. (2002a) from the cosmic shear survey of Van Waerbeke et al. (2001), although they used a different estimator of the shear 3PCF. The S/N for one particular triangle configuration with size r scales roughly as $S/N \propto \zeta_\gamma(\sigma_\epsilon/\sqrt{n_{\rm gal}})^{-3}\Omega_{\rm survey}^{1/2} r^2(\Delta \ln r)^{3/2}$, where $\Omega_{\rm survey}$ is the survey area. By combining information from triangles with different configurations and from the different 3PCFs, we can improve the S/N (however, to interpret the measured 3PCFs one must estimate how correlated neighboring bins are, as discussed below). Note further that we have used the SCDM model with $\zeta_{+++} = 2-4\times10^{-6}$ for $r = 1-5'$; the S/N for the concordance ΛCDM model is lower because the signal is smaller, e.g. $\zeta_{+++} = 4-8\times10^{-7}$ (Takada & Jain 2002c). This rough analysis leads us to conclude that future surveys with area $\gtrsim 100$ degree^2 should provide measurements of the 3PCFs with S/N well over 10 in each bin if systematic errors are eliminated.

4. DISCUSSION

We have investigated the 3PCF of the cosmic shear field. We measured the eight components of the shear 3PCF from ray-tracing simulations and checked our results using analytical calculations based on the halo model. Figures 2 and 3 show that in general all eight components are non-zero, have comparable amplitude, and have a complex configuration dependence. These results verify the analysis of SL02 who analyzed the 3PCFs based on their transformations under parity and rotations.

The 3PCFs show non-Gaussian signatures induced by nonlinear gravitational clustering. In constraining models from measurements of the shear 3PCFs, it will be necessary to develop an optimal way to combine the eight 3PCFs. To do this, we will need explicit relations showing how the shear 3PCFs are related to the lensing E-mode, in analogy with two-point statistics (Crittenden et al. 2001; Schneider et al. 1998, 2002). This problem is more easily formulated in Fourier space. If we use the Cartesian components of the shear to define the 3PCFs, then simple relations exist between the bispectra of the shear 3PCFs, $\tilde\zeta_{ijk}$ and the bispectrum of the convergence, B_κ:

$$\tilde\zeta_{ijk}(\mathbf{l}_1,\mathbf{l}_2,\mathbf{l}_3) = B_\kappa(\mathbf{l}_1,\mathbf{l}_2,\mathbf{l}_3)u_i(\mathbf{l}_1)u_j(\mathbf{l}_2)u_k(\mathbf{l}_3), \qquad (8)$$

where $i,j,k = 1,2$ and $u_i(\mathbf{l}) = (\cos2\varphi_\mathbf{l}, \sin2\varphi_\mathbf{l})$ for the E-mode. This equation shows that the shear 3PCFs can be related to a single 3PCF for the E-mode field. For example we can obtain the convergence bispectrum using the eight measured shear bispectra as:

$$B_\kappa(\mathbf{l}_1,\mathbf{l}_2,\mathbf{l}_3) = \sum_{i,j,k} u_i(\mathbf{l}_1)u_j(\mathbf{l}_2)u_k(\mathbf{l}_3)\tilde\zeta_{ijk}(\mathbf{l}_1,\mathbf{l}_2,\mathbf{l}_3). \qquad (9)$$

However in real space it is still unclear how best to use the eight 3PCFs measured over a limited range of scales to get an optimal estimator of the E-mode 3PCF. Another question we have not considered is how strongly the shear 3PCFs are correlated for different triangle configurations, since lensing fields at arcminute scales are highly non-Gaussian (e.g. Takada & Jain 2002a).

Realistic data has noise which includes both E/B modes, as would contributions from intrinsic ellipticity correlations, nonlinear lensing effects and systematic errors. We have shown that two or all four parity-odd 3PCFs vanish for isosceles or equilateral triangles, respectively (see Figures 2 and 4). For general triangles, Figure 3 shows that the 3PCFs of E-mode shear fields have specific symmetry properties under the change $\psi \to 2\pi - \psi$, where ψ is the interior angle of the triangle shown in Figure 1. These properties can be used to find B-mode contributions (whose symmetry properties are reversed) as a function of scale and configuration. Thus the origin of the B-mode contribution can be identified more precisely than is possible with two-point statistics. An example of an explicit test for B modes is to measure combinations such as $\zeta_{++\times}(x_1,x_2,\psi) + \zeta_{++\times}(x_1,x_2,2\pi-\psi)$. This should be zero for all the functions that are parity-odd for a pure E mode, as given in equation (3).

The results presented above can also be applied to the Q and U Stokes parameters of the CMB polarization. The results we have shown imply that the eight 3PCFs constructed from combinations of Q/U, e.g. $\langle UQQ\rangle$, have non-vanishing signals if the CMB polarization field is non-Gaussian. The 3PCFs have the advantage that it can discriminate the non-Gaussianity arising from the E- and B-modes. However, since the polarization signal is small compared to the CMB temperature fluctuations, this will be a great challenge.

We are grateful to G. Bernstein, L. Hui, M. Jarvis, P. Schneider, R. Scoccimarro, A. Stebbins, A. Szalay and M. Tegmark for helpful discussions. This work is supported by NASA grants NAG5-10923, NAG5-10924 and a Keck foundation grant.

REFERENCES

Barriga, J., & Gaztañaga, E. 2002, MNRAS, 333, 443
Bartelmann, M., & Schneider, P. 2001, Phys. Rep. 340, 291
Bernardeau, F., Mellier, Y., & Van Waerbeke, L. 2002a, A&A, 389, L28
Bernardeau, F., Van Waerbeke, & L., Mellier, Y. 2002b, astro-ph/0201029
Crittenden, R. G., Natarajan, P., Pen, U.-L., & Theuns, T. 2001, ApJ, 559, 552
Hu, W., & White, M. 1997, Phys. Rev. D, 56, 596
Jain, B., Seljak, U., & White, S. D. M. 2000, ApJ, 530, 547
Kaiser, N. 1992, ApJ, 388, 272
Kamionkowski, M., Kosowsky, A., & Stebbins, A. 1997, Phys. Rev. D, 55, 7368
Kamionkowski, M., Babul, A., Cress, C. M., & Refregier, A. 1998, MNRAS, 301, 1064
Komatsu, E., Wandelt, B. D., Spargel, D., Banday, A. J., & Górski, K. M. 2002, ApJ, 566, 19
Schneider, P., & Lombardi, M. 2002, astro-ph/0207454 (SL02)
Schneider, P., Van Waerbeke, Jain, B., & Kruse, G. 1998, MNRAS, 296, 873
Schneider, P., Van Waerbeke, L., Kilbinger, M., & Mellier, Y. 2002, astro-ph/0206182
Stebbins, A., 1996, astro-ph/9609149
Takada, M., & Jain, B. 2002a, MNRAS, in press, astro-ph/0205055
Takada, M., & Jain, B. 2002b, submitted to MNRAS, astro-ph/0209167
Takada, M., & Jain, B. 2002c, in preparation

Van Waerbeke et al. 2001, A&A, 374, 757
Verde, L., Wang, L., Heavens, A. F., & Kamionkowski, M. 2000, MNRAS, 313, 141
Zaldarriaga, M., & Scoccimarro, R. 2002, astro-ph/0208075 (ZS02)
Zaldarriaga, M., & Seljak, U. 1997, Phys. Rev. D, 55, 1830